Inorganic Chemistry

Article

pubs.acs.org/IC

Platinum(II) Monomer and Dimer Complexes with a Bis(oxazolinyl)phenyl Pincer Ligand

Daoli Zhao, Jeanette A. Krause, and William B. Connick*

Department of Chemistry, University of Cincinnati, P.O. Box 210172, Cincinnati, Ohio 45221-0172, United States

Supporting Information

ABSTRACT: A series of platinum(II) complexes with the formulas $Pt(phebox)(L)^+$ ($phebox^-$ = 1,3-bis(4,4′-dimethyl-2′-oxazolinyl)phenyl anion; L = pyridine (py), 4-phenylpyridine, quinoline, acridine) and $Pt_2(phebox)_2(\mu\text{-}L')^{2+}$ (L′ = pyrazine, 4,4′-bipyridine, 1,2-bis(4-pyridyl)ethane) was prepared. Crystallographic data establish that the metal center is bonded to the tridentate $phebox^-$ and monodentate pyridyl ligands. The five-membered oxazoline rings favor a CH_2-CMe_2 twist conformation. $Pt(phebox)Cl$ and $Pt(phebox)(py)^+$ undergo a ligand-based chemically reversible redox reaction, whereas the electrochemistry of the other complexes is chemically and electrochemically less reversible. In contrast to complexes with the 1,3-bis(piperdylmethyl)phenyl anion ligand (pip_2NCN^-) or related pincer ligands, each of the $phebox^-$ complexes described here exhibits intense emission in room-temperature methylene chloride solution, which is assigned as originating from a lowest, predominantly $phebox^-$ ligand-centered excited state. In acetonitrile, the complexes undergo solvolysis resulting in displacement of the pyridyl ligands. The accumulated data demonstrate that subtle variations in the nature of the NCN and ancillary ligands of platinum(II) complexes provide access to at least five orbitally distinct emissive excited states.

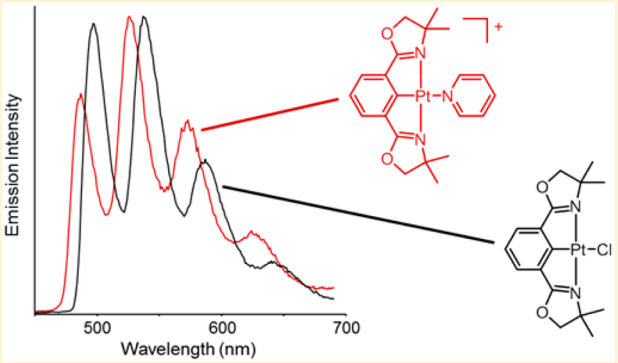

INTRODUCTION

Cyclometalated platinum(II) complexes with tridentate pincer type ligands, especially NCN complexes, have attracted widespread interest because of their potential to function as catalysts for allylation,[1−7] Diels−Alder reactions,[8] Michael addition,[9−12] aldol reactions,[13,14] hydrosilylation,[15] conjugate reduction,[16−18] and Heck reactions,[19−22] as well as hydrogenation of ketones.[23] There also is growing interest in these systems because of their intriguing photophysical properties and potential application in optoelectronic devices such as organic light-emitting devices[24] and chemical sensors.[25] One interesting class of compounds is composed of $Pt(R_4NCN)(L)^{n+}$ complexes, such as $Pt(Me_4NCN)Cl$, which were developed by van Koten and co-workers (Scheme 1).[1,26,27] In a series of previous studies, we reported the structural and electronic properties of a series of $Pt(pip_2NCN)(L)^{n+}$ monomers (L = halide, pyridyl ligand, n = 0, 1) and $Pt_2(pip_2NCN)_2(\mu\text{-}L')^{2+}$ (L′ = bridging pyridyl ligands).[28−30] Variations in the ancillary L ligand were shown to provide exquisite control over the electronic structures and luminescence properties of these complexes, allowing for tuning of the emission maximum from 430 to 640 nm. For example, the emission from $Pt(pip_2NCN)(L)^{n+}$ originates from a predominantly spin-forbidden ligand field state when L = py or halide, whereas the emission originates from a lowest pyridyl ligand-centered state (^{3}LC) when L is 4-phenylpyridine or L′ is 4,4′-bipyridine in the case of $Pt_2(pip_2NCN)_2(\mu\text{-}L')^{2+}$. When L′ is a bridging pyrazine (pyz), the emission has significant triplet metal-to-ligand (pyz) charge-transfer (^{3}MLCT) character. These conclusions also are consistent with density functional theory (DFT) calculations,[31] which suggest that MLCT states

Scheme 1. Selected NCN Pincer Ligands

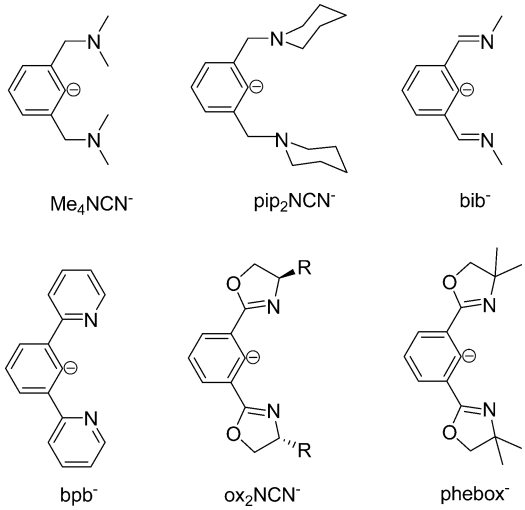

Received: May 6, 2015

DOI: 10.1021/acs.inorgchem.5b01022
Inorg. Chem. XXXX, XXX, XXX−XXX

Scheme 2. Syntheses of Platinum(II) Monomer and Dimer Complexes

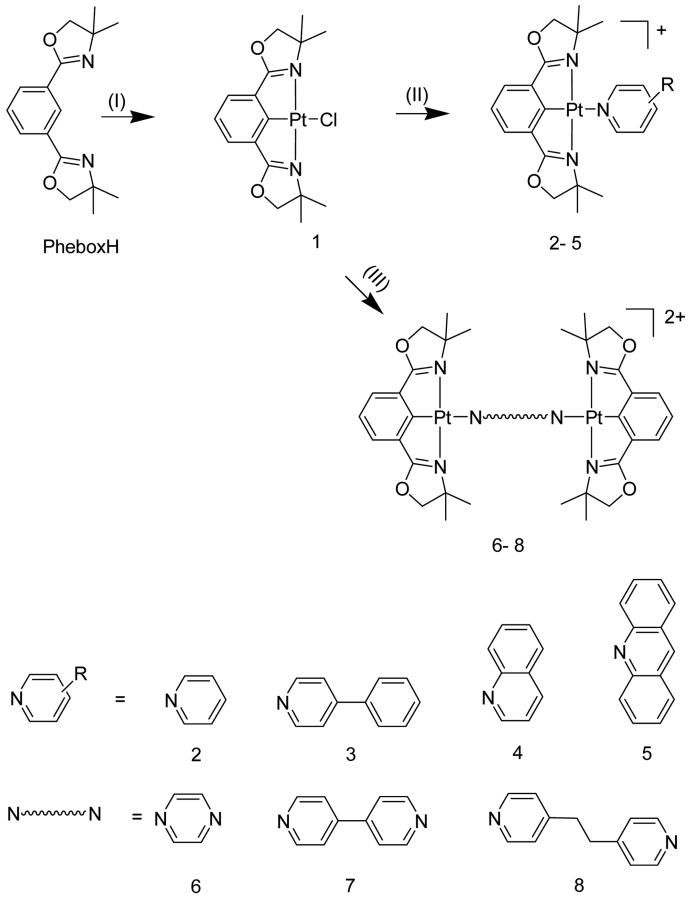

Conditions: (I) K_2PtCl_4, acetic acid, (II) silver salt, pyridyl ligand, (III) silver salt, bridging pyridyl ligand

involving the bridging L′ ligand are stabilized by introduction of either electron-releasing substituents on the phenyl group of the NCN ligand or electron-withdrawing substituents on L′, as well as by extending the length of the conjugated bridging ligand. Though the preceding systems are essentially non-emissive in room-temperature (RT) solution, Batema et al. have elegantly demonstrated that Pt(Me_4NCN)Cl complexes exhibit intense fluid-solution fluorescence when functionalized with a 4′-substituted styryl group.[32] The resulting stilbene group largely retains its luminescence properties albeit with decreased quantum yield due to the attached platinum center.

Complexes with the chiral bis(oxazolinyl)phenyl ligand (ox_2NCN^-; Scheme 1) were developed by Nishiyama,[5] Denmark,[21] and Richard[22] and have been extensively studied as catalysts for asymmetric synthesis.[4,5,19,20,33−37] Despite considerable interest in the chemistry of platinum complexes with this class of NCN ligand, there have been no reports on the luminescence properties of platinum(II) complexes with oxazoline pincer ligands, and comparatively little is known about their electronic structures. However, there have been reports on the luminescence properties of related NCN complexes with imine groups, such as Pt(bib)Cl (bibH = 1,3-bis(*N*-methylimino)benzene)[38] and Pt(bpb)Cl (bpbH = 1,3-bis(2-pyridyl)benzene) (Scheme 1).[39−41] For example, Pt(bib)Cl exhibits RT emission in CH_2Cl_2 solution assigned to a lowest state with mixed MLCT and ligand-to-ligand charge-transfer (LLCT) character with the lowest unoccupied molecular orbital mainly localized on the tridentate ligand. Emissions from Pt(bpb)Cl and Pt(bpb)(C≡N(C_6H_3-2,6-Me_2))$^+$ have been assigned as originating from a mixed LC/MLCT state.[39−43] Understanding of the electronic structures of such systems is expected to guide efforts to tailor the optical properties and reactivity of these systems. Because of the relative basicities (e.g., pK_b values: oxazoline, 4.70; piperidine, 11.12)[44,45] and π-acidities of the N-donor groups, the comparatively rigid ox_2NCN^- ligand is reasonably expected to be a slightly weaker σ-donor and much stronger π-acceptor than either Me_4NCN^- or pip_2NCN^-. Therefore, MLCT states involving the lowest π^* level of ox_2NCN^-, as well as pincer LC states with ox_2NCN^- $\pi-\pi^*$ character, are expected to be stabilized. To assess the influence of the oxazoline groups on the molecular geometries, electronic structures, and spectroscopic properties of platinum complexes with NCN ligands, we undertook the synthesis and characterization of a series of monomer and dimer complexes with the phebox$^-$ ligand (Scheme 1): Pt(phebox)(L)$^{n+}$ (L = Cl, pyridyl ligand) and Pt_2(phebox)$_2$(μ-L′)$^{2+}$ (L′ = bridging pyridyl ligand). In contrast to their pip_2NCN^- counterparts, the complexes are emissive in RT fluid solution.

EXPERIMENT SECTION

K_2PtCl_4 was obtained from Pressure Chemical Co. 1,3-Dicyanobenzene and $AgBF_4$ were obtained from Sigma-Aldrich. $AgPF_6$ was obtained from Alfa Aesar. All other reagents were purchased from Acros. Glacial acetic acid was dried by distilling from P_2O_5 and acetic anhydride. Methylene chloride was distilled over CaH_2. Tetrabutylammonium hexafluorophosphate ($TBAPF_6$) was recrystallized three times from boiling ethanol and dried under vacuum prior to use. All

DOI: 10.1021/acs.inorgchem.5b01022
Inorg. Chem. XXXX, XXX, XXX−XXX

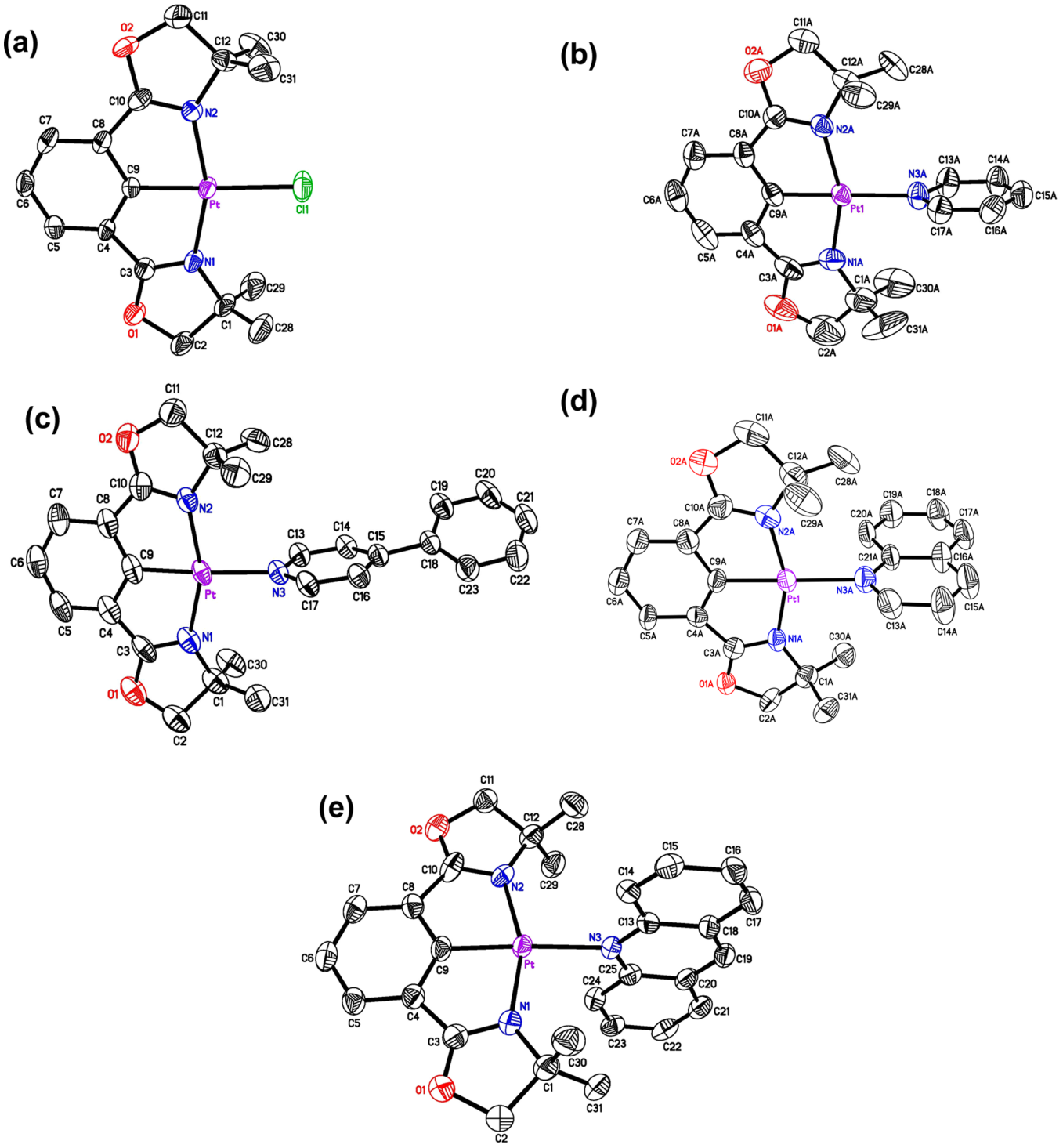

Figure 1. ORTEP diagram of the cations in crystals of the Pt(phebox)(pyridyl)$^+$ monomers: (a) **1**, (b) Molecule A of **2b**, (c) **3-m**, (d) Molecule A of **4**·3/4C_6H_{14}·1/2H_2O, and (e) **5**. Ellipsoids plotted at 50% probability, H atoms omitted for clarity. (ORTEP diagrams of the cations of Molecule B for **2b**, **3-o**, and **4**·3/4C_6H_{14}·1/2H_2O are in Figure S1).

other chemicals were used as received. Pt(phebox)Cl (**1**) was prepared as previously described.[34] Argon was predried using activated sieves, and trace oxygen was removed with activated R3−11 catalyst from Schweizerhall. The synthesis of 1,3-bis(4,4′-dimethyl-2-oxazolinyl)-benzene (pheboxH) and its metal complexes is described in the Supporting Information.

^{1}H NMR spectra were recorded at RT using a Bruker AC 400 MHz instrument. Deuterated solvents $CDCl_3$ (0.03% (v/v) tetramethylsilane (TMS)) and CD_3CN were purchased from Cambridge Isotope Laboratories. Spectra are reported in parts per million (ppm) relative to TMS (δ = 0 ppm) for $CDCl_3$ or relative to the protic solvent impurity in the case of CD_3CN (δ = 1.94 ppm for CD_2HN). Elemental analyses were performed by Atlantic Microlab, Inc. (Norcross, GA). UV−visible absorption spectra were recorded using a HP8453 UV−visible diode array spectrometer. Emission spectra were recorded using a SPEX Fluorolog-3 fluorimeter equipped with a double-emission monochromator (385 nm cutoff filter) and a single excitation monochromator. Glassy solutions (77 K) were prepared by inserting a quartz electron paramagnetic resonance tube containing a 4:1 ethanol−methanol solution of the respective complex into a

DOI: 10.1021/acs.inorgchem.5b01022
Inorg. Chem. XXXX, XXX, XXX−XXX

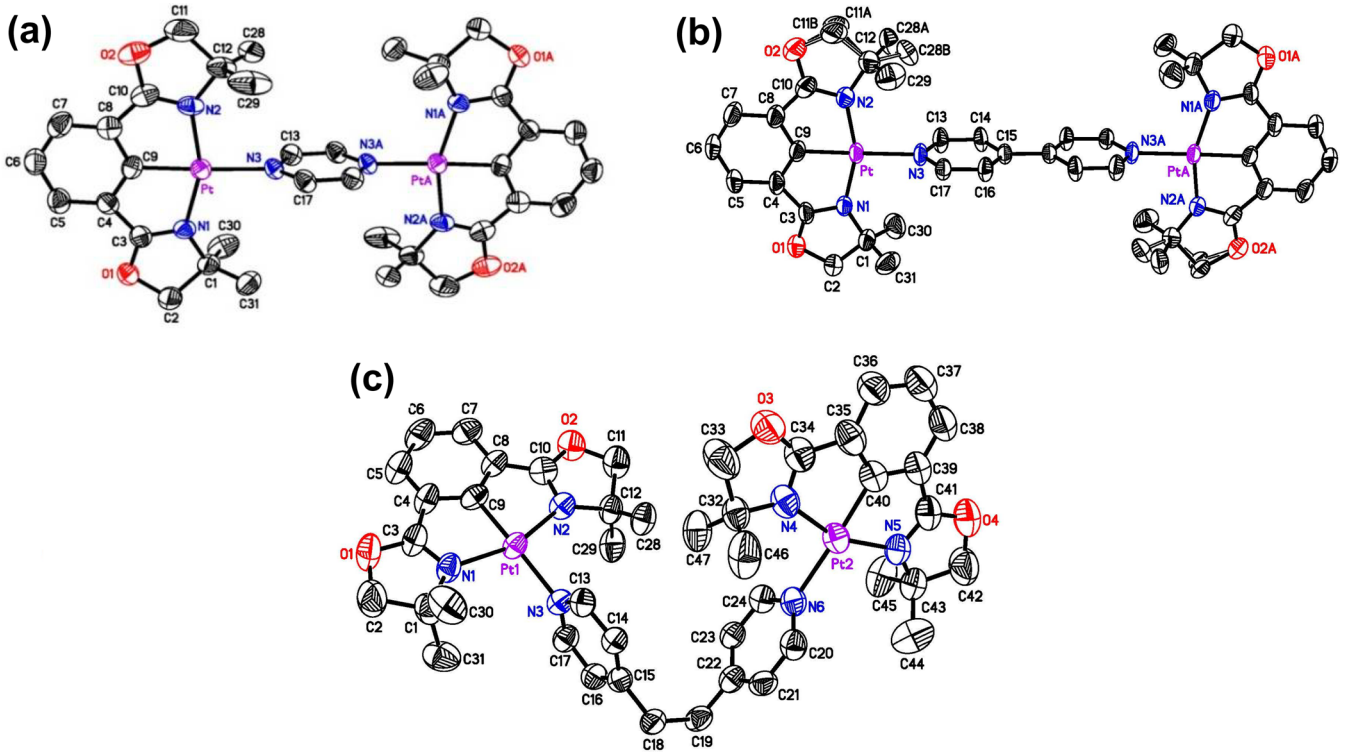

Figure 2. ORTEP diagram of the cations in crystals of $Pt_2(phebox)_2(\mu\text{-}L')^{2+}$ (a) **6**·$2C_3H_6O$, (b) **7b**·$2C_3H_6O$ and (c) **8-c**·$C_4H_{10}O$. Ellipsoids plotted at 50% probability. H atoms omitted for clarity. (ORTEP diagram of the cation in **8-p**·$5/4C_3H_6O$ is in Figure S1).

quartz-tipped finger Dewar. Emission spectra were corrected for instrumental response. Mass spectra were obtained by electrospray ionization (ESI) of acetonitrile or methanol solutions using a Micromass Q-TOF-2 instrument. Experimental details of the crystallography, as well as selected metrics for the complexes, are provided in the Supporting Information.

Cyclic voltammetry measurements were performed using a standard three-electrode cell and a 100 B/W electrochemical workstation from Bioanalytical Systems. Scans were recorded of 1−1.5 mM CH_2Cl_2 solutions containing 0.1 M $TBAPF_6$. All scans were recorded using a platinum wire auxiliary electrode and a 0.79 mm^2 platinum working electrode. Between measurements, the working electrode was polished with 0.05 μm alumina, rinsed with distilled water, and wiped dry using a Kimwipe. Reported potentials are referenced versus Ag/AgCl (3.0 M NaCl). Peak currents (i_p) were estimated with respect to the extrapolated baseline current, as described by Kissinger and Heineman.[46] Under these conditions, the ferrocenium/ferrocene (Fc^+/Fc) couple occurs at 0.50 V. The values of $(E_{pc} + E_{pa})/2$, which is an approximation of the formal potential for a redox couple, are referred to as $E^{\circ\prime}$.

RESULTS AND DISCUSSION

Synthesis and Characterization. The preparation of protonated oxazoline pincer ligand precursors, such as pheboxH, has typically been accomplished in four steps, using thionyl chloride in a moisture-free environment.[47] Although Button and co-workers reduced the synthesis to two steps using anhydrous $ZnCl_2$, the preparation of the catalyst is cumbersome, requiring three cycles of crystallization from a melt under vacuum and cooling under Ar.[48] We found that pheboxH is readily prepared in a single step by refluxing 1,3-dicyanobenzene and 2-methyl-2-amino-1-propanol in the presence of $Zn(OAc)_2·2H_2O$ in air without prior drying or purification of the solvent. Using this product, Pt(phebox)Cl was prepared as previously described.[34] From that complex, a series of monomers and dimers with the $phebox^-$ pincer ligand were readily prepared by treatment with a slight excess of a soluble silver(I) salt, followed by addition of a pyridyl ligand (Scheme 2). The complexes were isolated as the pale yellow hexafluorophosphate salts. In the cases of the pyridyl and bipyridyl complexes, both the PF_6^- (**2a** and **7a**) and the BF_4^- (**2b** and **7b**) salts were prepared. The products were characterized by a combination of ^1H NMR spectroscopy, elemental analysis, mass spectrometery, and X-ray crystallography. The salts are soluble in polar organic solvents (e.g., dichloromethane) but readily undergo solvolysis in acetonitrile resulting in displacement of the pyridyl ligand (vide infra). With the exception of **4**, the patterns of resonances in the ^1H NMR spectra are consistent with C_{2v} symmetric complexes, indicating that any distortion of the five-membered oxazolinyl ring is not long-lived. However, at RT, the $phebox^-$ methyl protons of **4** appear as two equally intense resonances (rather than a single resonance), indicating that rotation of the quinoline ligand about the Pt−N bond is slow. The α-protons of the pyridyl/pyrazinyl ligand occur at ≥8.5 ppm, significantly shifted downfield from those of the free ligand. Similarly, the methyl proton resonance for **1** is shifted by 0.3 ppm downfield from the free ligand resonances. By contrast, the methyl resonances are shifted 0.2−0.8 ppm upfield in the spectra **2**−**8** due to the ring current of the nitrogen heterocycle.

Structures. The structures of **1**−**8** were confirmed by X-ray crystallography (Figures 1, 2, and S1; Tables S1−S4). Each platinum center is bonded to a tridentate $phebox^-$ ligand and a pyridyl ligand, resulting in a distorted square planar coordination geometry similar to those found for other platinum(II) complexes with oxazolinyl pincer ligands.[20,33,34,49] The pyridyl groups are approximately perpendicular to the coordination plane, as expected for the steric demands of the oxazoline methyl groups, whose proximity

DOI: 10.1021/acs.inorgchem.5b01022
Inorg. Chem. XXXX, XXX, XXX−XXX

restricts rotation of the pyridyl group about the Pt−N bond and results in upfield shifts in the ^{1}H NMR spectra. The intramolecular Pt···Pt distances for dimers **6** (7.0285(5) Å), **7b** (11.3489(8) Å), and **8-c** (9.1385(6) Å) and **8-p** (9.1884(6) Å) are typical for these bridging ligands.[29,30,50−58] In crystals of **8-p** and **8-c**, the 1,2-bis(4-pyridyl)ethane (bpa) ligand adopts the less energetically favorable gauche conformation, presumably due to packing effects. It is interesting that the Pt−N(pyridyl) bond lengths for **1**−**8** are significantly shorter than those found for pip_2NCN^- analogues,[29,30] as well as $Pt(Me_4NCN)(pyOH)^+$.[59,60] The accumulated data indicate a stronger interaction between the platinum center and pyridyl ligand in the phebox$^-$ series and suggests that phebox$^-$ is a weaker trans/cis directing ligand than pip_2NCN^- or Me_4NCN^-.

We also note that the puckering of the five-membered oxazolinyl rings for these and seven related complexes was characterized based on previously developed descriptions of five-member rings (Supporting Information).[20,33,34,49] Those results show that the oxazolinyl groups do not lie on a single pseudorotation pathway with a unique puckering amplitude and that complexes with large puckering amplitudes show a decided preference for a CH_2-CMe_2 twist conformation.

Electrochemistry. To better understand the electronic structures of these complexes, cyclic voltammograms (CVs) were recorded in 0.1 M $TBAPF_6$ methylene chloride solution (Table 1). None of the complexes showed oxidation waves at <1.5 V versus Ag/AgCl. However, excepting **5**, each of the monomers exhibited a reduction wave in the −1.3 to −1.5 V range, which is tentatively assigned to a phebox$^-$ ligand-based process. Notably, the ∼0.12 V anodic shift of the pyridine complex relative to **1** is consistent with the expected relative donor properties of the ancillary pyridyl and chloro ligands; similar shifts occur for the mainly polypyridyl ligand-based reductions of $Pt(tpy)L^{n+}$ (0.22 V; tpy = 2,2′:6′,2″-terpyridine),[61] $Ru(tpy)(2,2'\text{-bpy})L^{n+}$ (0.20 V; 2,2′-bpy = 2,2′-bipyridine),[62] and $Ru(2,2'\text{-bpy})_2(Cl)(L)$ (0.11 V).[63] Also in keeping with this assignment, we note that **2**−**4** and **8** were reduced at more positive potentials than the chloro complex (**1**). An interesting comparison comes from the observation that the reduction process for **1** (−2.0 V vs Fc^+/Fc) is shifted by 0.1−0.3 V to more positive potentials compared to that of Pt(bpb)Cl (CH_2Cl_2, −2.14 V; dimethylformamide (DMF), −2.18 V vs Fc^+/Fc)[64] and Pt(Mebpb)Cl (Mebpb$^-$ = 5-methyl-1,3-di(2-pyridyl)phenyl anion; CH_2Cl_2, −2.27 V vs Fc^+/Fc),[65] despite the expected increased delocalization in these latter systems. By contrast, cationic $Pt(tpy)Cl^+$ is reduced at significantly more positive potentials (DMF: −0.74 V vs Fc^+/Fc), in keeping with its positive charge and strong tpy(π*)/Pt($6p_z$) mixing.[61] Therefore, we conclude that the first reduction potentials follow the order $Pt(tpy)Cl^+ \gg$ Pt(phebox)Cl > Pt(Mebpb)Cl.

Table 1. Electrochemical Data for $Pt(phebox)L^{n+}$ (1−5) and $Pt_2(phebox)_2(\mu\text{-}L')^{2+}$ (6−8)

L (compound no.)	$E°'$, V (ΔE_p, mV)[a]
Cl (**1**)	−1.50 (100)
py (**2a**)	−1.38 (85)
phpy (**3**)	−1.46 (67)
quin (**4**)	−1.31 (100)
ac (**5**)	−1.19 (irr)
pyrazine (**6**)	−0.79 (80)
bpy (**7a**)	−1.07 (80), −1.49(140)
bpa (**8**)	−1.33 (100)

[a]Cyclic voltammograms were recorded in 0.1 M $TBAPF_6/CH_2Cl_2$ at 0.10 V/s and referenced vs Ag/AgCl.

By contrast, compounds **5**−**7** undergo pyridyl ligand-based reductions at greater than −1.3 V. For example, the −1.19 V anodic peak potential for **5** is close to that observed for protonated acridine (−1.20 V; 1 M KNO_3 in 0.01 M HCl).[66] The bridging ligand reduction processes for **6** and **7** are nearly reversible and anodically shifted by ∼0.1 V from those of their $Pt_2(pip_2NCN)_2(\mu\text{-}L)^{2+}$ counterparts (pyz: −0.88 V, ΔE_p = 66 mV;[30] bpy: −1.07 V, ΔE_p = 80 mV). Thus, it is evident that the $Pt(phebox)^+$ unit has a slightly stronger stabilizing effect on the bridging ligand π* level than $Pt(pip_2NCN)^+$. This observation is consistent with the notion that the weaker σ-donor and stronger π-acceptor properties of phebox$^-$ conspire to make it an overall weaker donor than pip_2NCN^-.

Electronic Spectroscopy. The electronic spectrum of **1** exhibits maxima near 295, 340, and 380 nm (∼5000 M^{-1} cm^{-1}; Figure 3 and Table S5), spanning a region where pheboxH absorbs only weakly. The two longest wavelength maxima occur in a region where transitions with significant MLCT and/or phebox LC character are expected.[38−42,64] Both bands are somewhat solvent-sensitive, shifting to longer wavelength with decreasing polarity (Figure S5). The longer wavelength transition near 380 nm likely has significant MLCT character because it is absent from the spectra of **2**−**4** and **6**−**8**, presumably because it is shifted by at least 1300 cm^{-1} to shorter wavelength (Figures 3 and S5). This is consistent with the expectation that MLCT states in the latter complexes lie at higher energy than in **1**, because the nitrogen heterocyclic ligands are weaker donors than the chloro ligand. For example, the longest wavelength MLCT band of $Ru(tpy)(bpy)Cl^+$ (550 nm) is red-shifted from that of $Ru(tpy)(bpy)(py)^{2+}$ (465 nm) by 1500 cm^{-1}.[62]

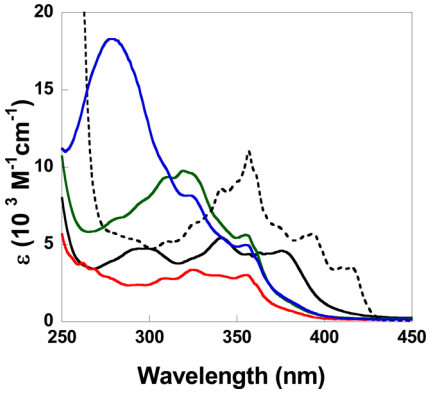

Figure 3. RT electronic absorption spectra of **1** (black), **2** (red), **3** (blue), **4** (green), and **5** (dashed line) in CH_2Cl_2.

For comparison, we note that the electronic spectrum of Pt(bib)Cl exhibits two longest wavelength absorption band maxima at 386 (4.1×10^3 M^{-1} cm^{-1}) and 400 nm (4.4×10^3 M^{-1} cm^{-1}).[38] Similarly, Pt(bpb)Cl shows two long-wavelength bands at 380 (8.7×10^3 M^{-1} cm^{-1}) and 401 nm (7.0×10^3 M^{-1} cm^{-1}).[39] Several studies of these and related complexes with substituted bpb$^-$ ligands support the consensus view that several bands having significant LC(π−π*) and MLCT character occur in this region with the longest wavelength band having substantial MLCT character.[39−42,64] For six

DOI: 10.1021/acs.inorgchem.5b01022
Inorg. Chem. XXXX, XXX, XXX−XXX

solvents investigated, the 340 and 380 nm bands in the spectrum of Pt(phebox)Cl are approximately twice as sensitive as the band maxima for Pt(bpb)Cl, in keeping with the notion that the 380 nm band of **1** also has significant MLCT character. From these comparisons and the spectrum of $Pt(tpy)Cl^+$ (405 nm),[67] it is evident that the relative energies of the lowest spin-allowed MLCT states are Pt(phebox)Cl > Pt(bib)Cl ≈ Pt(bpb)Cl ≈ $Pt(tpy)Cl^+$. The similarity in energies for the latter three compounds is attributable to several factors. First, the results suggest that the marked stabilization of the π^*(tpy) level of $Pt(tpy)Cl^+$ (vide supra) is largely offset by stabilization of the Pt 5d orbitals due to reduced donation by the tridentate tpy ligand, as compared to NCN ligands. Likewise, although the π-system of Pt(bib)Cl is smaller than that of Pt(bpb)Cl, the strong π-acceptor properties of the imine groups of Pt(bib)Cl are expected to stabilize MLCT states, as noted for pyridine carboxaldimine complexes.[68] However, the ∼0.15 eV destabilization of the lowest ^{1}MLCT state of **1** as compared to Pt(bib)Cl is attributable to the relative donor properties of the ether and methyl substituents on the ligand π^* level. An additional consideration is variation in the extent of LC/MLCT mixing, though detailed knowledge of this effect is currently lacking.

At long wavelengths, the absorption profiles of the dimers (**6**–**8**; Figure S6) are similar to those of **2**–**4**. For example, the spectrum of **8** is almost identical to that of $Pt(phebox)(py)^+$ (**2**) except with ∼1.5 times the molar absorptivity. This is consistent with the notion that the electronic structures of the $Pt(phebox)(pyridyl)^+$ and $Pt(phebox)(pyz)^+$ units are only weakly unperturbed by dimer formation. Also note that **6** (257 nm, 13.3 × 10^3 M^{-1} cm^{-1}) and **7** (268 nm, 15.3 × 10^3 M^{-1} cm^{-1}) exhibit shorter wavelength bands tentatively assigned to bridging ligand transitions.[29,30,69,70] Likewise, compounds **3** and **4** also show contributions from the N-heterocyclic ligands at $\lambda \leq 320$ nm, which are found in spectra of related molecules.[29,71−76] At wavelengths greater than 320 nm, the absorption profile of **5** is distinctly different and more intense than that observed for the other compounds; the observed progression in the 330−360 nm range and the band at 415 nm also appear in the spectrum of acH^+.[77]

Ligand Dissociation. Whereas compound **1** is stable in acetonitrile, **2**–**8** are not, and the observed behavior is consistent with solvolysis resulting in displacement of the pyridyl ligands. This is illustrated for **3** by the reaction

$$Pt(phebox)(phpy)^+ + CH_3CN \leftrightarrows Pt(phebox)(NCCH_3)^+ + phpy \quad (1)$$

For example, in RT ∼2 mM CD_3CN solutions, the pyridyl resonances in the ^{1}H NMR spectra of **3** were coincident with those of the free ligand, indicating that the ligand was fully dissociated. The pattern of $phebox^-$ resonances is consistent with formation of C_{2v} symmetric $Pt(phebox)(CD_3CN)^+$, which was also identified in the mass spectrum. Notably, the oxazoline CH_2 and $C(Me)_2$ proton resonances appeared at 4.76 and 1.49 ppm, respectively. Coordination of acetonitrile was suggested by the downfield shift of the solvent CD_2HCN resonance. With the addition of pyridine (Figure S7), a new set of resonances appeared, including the α-proton resonance of coordinated pyridine at 9.00 ppm and a new set of CH_2 and $C(Me)_2$ proton resonances at 4.66 and 1.10 ppm, respectively. Evaporation of the solvent and recording of the ^{1}H NMR spectrum in CD_2Cl_2 confirmed complete recovery of the original $Pt(phebox)(phpy)^+$ complex.

Titration of a methylene chloride solution of **3** with acetonitrile showed a gradual decrease in intensity of the phpy-centered 278 nm absorption band, confirming ligand dissociation (Figure 4). The absence of large changes at >330 nm is consistent with this region being dominated by mainly transitions involving the $phebox^-$ ligand in the $Pt(phebox)(phpy)^+$ and $Pt(phebox)(CH_3CN)^+$ complexes (Figure 4). During titration with acetonitrile (0−45% by volume), isosbestic points were not well-defined, presumably because of the sensitivity of the spectra to changes in solvent dielectric. Under the assumption of the solvolysis equilibrium in eq 1, the equilibrium constant was estimated to be ∼2 × 10^{-4}, indicating a strong preference for coordination of phpy over acetonitrile.

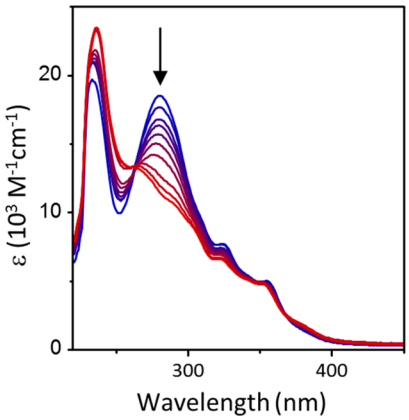

Figure 4. Apparent molar absorptivity (ε) of a 70 μM solution of $Pt(phebox)(phpy)^+$ in methylene chloride during titration with 1.2 × 10^5 equiv of acetonitrile.

Emission Spectroscopy. Whereas $Pt(pip_2NCN)(L)^+$ complexes are essentially nonemissive in fluid solution, compounds **1**–**8** exhibit intense yellow-orange emission in methylene chloride solution. Thus, the influence of the more conjugated NCN ligand is immediately obvious. Lowest-lying excited states in such systems have been extensively discussed,[29,38−42,64,78,79] and the most logical candidates in the present case are those with LC and/or MLCT character involving the $phebox^-$ ligand; excited-state mixing will be favored when the parent states approach in energy and there is strong metal−ligand interaction. Consistent with this notion, we note that the 1400−1500 cm^{-1} vibronic spacings in the emission profile of Pt(phebox)Cl are indicative of involvement of the $phebox^-$ ligand (Figure 5a and Table 2). The emission lifetime is concentration-dependent, consistent with bimolecular self-quenching, as noted previously for platinum polypyridyl complexes.[80] Presumably because of the steric demands of the oxazolinyl methyl substituents, the self-quenching rate constant (k_{sq}, 1.7(3) × 10^9 M^{-1} s^{-1}) is slightly less than that found for Pt(bpb)Cl (k_{sq}, 5.3 × 10^9 M^{-1} s^{-1}).[40] The lifetime at infinite dilution (3.0(1) μs) confirms that the emission originates from a predominantly spin-forbidden excited state. With the exception of **5**, the structured emission profiles of the remaining compounds are nearly superposable with 1400−1500 cm^{-1} vibronic spacings similar to those of **1**. However, as compared to the spectrum of **1**, the emission band is shifted by ∼800 cm^{-1} to longer wavelength. In other words, it is evident that the emission energy is mildly sensitive to the donor properties of the ancillary ligand (e.g., Cl^- vs pyridine), which is consistent with a predominantly ^{3}LC excited state with partial MLCT

DOI: 10.1021/acs.inorgchem.5b01022
Inorg. Chem. XXXX, XXX, XXX−XXX

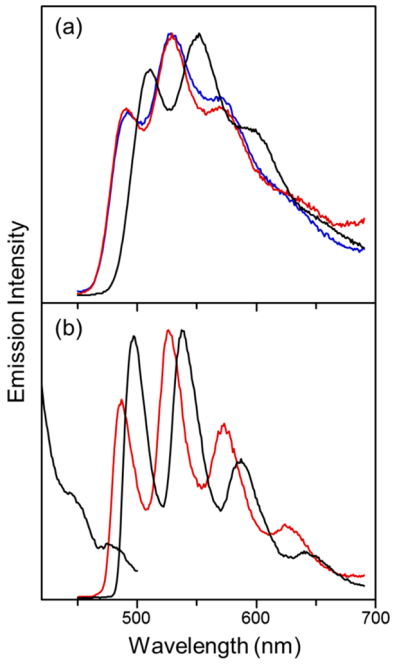

Figure 5. (a) Emission spectra of **1** (black), **2** (red), and **3** (blue) in RT CH_2Cl_2 solution and (b) emission spectra of **1** (black) and **2** (red, with excess pyridine), as well as the excitation spectrum of **1** (red), in 77 K 4:1 ethanol/methanol glassy solution.

Table 2. Emission Spectroscopic Data for 1−5 and 8 in Room-Temperature CH_2Cl_2 Solution (λ_{ex} = 350 nm)

compound	emission (λ_{max}, nm)	$I_{0,0}/I_{1,0}$ (S)
1	510, 552, 600 (sh), 654 (sh)	1.2
2a	490, 528, 570(sh), 629 (sh)	1.4
3	490, 529, 570(sh), 629(sh)	1.4
4	490, 527, 570(sh), 629(sh)	1.4
5	491, 530, 570(sh), 629 (sh)	
8	491, 532, 575(sh), 632(sh)	1.4

character. In support of this assignment, we note that the Huang−Rhys ratio ($S = I(1,0)/I(0,0)$) increases from 1.2 to 1.4 upon substitution of the chloro donor ligand with the more weakly donating N-heterocycle ligands, indicating an increase in the excited-state geometric distortion. For platinum(II) polypyridyl complexes having emissive states with mixed LC/MLCT character, the tendency of S to increase with increasing LC character is well-documented.[79] For example, the Huang−Rhys ratios for the chloro and cyano derivatives of $Pt(tpy)X^+$ in 77 K butyronitrile solution are 0.6 and 1.2, respectively.[67,81]

The vibronic structure is sharpened in 4:1 ethanol/methanol 77 K glassy solution, and the emission bands are slightly blue-shifted from the RT spectra (Figure 5b). Spectra of **2**−**4** under these conditions were excitation wavelength-dependent as expected for dissociation of the pyridyl ligand in alcohol solution (Figure S8); the resulting structured emission from $Pt(phebox)(ROH)^+$ (R = methyl, ethyl) occurs at slightly longer wavelength than that of the pyridyl complexes. To suppress ligand dissociation, spectra of the latter complexes were recorded with excess pyridyl ligand. The resulting spectra are distinctly sharper under these conditions and independent of excitation wavelength (Figure S9).[82] Similar to the RT results, the bands for **2**−**4** are red-shifted by 300−500 cm^{-1} from that of **1**. For comparison, MLCT emission from $Ru(tpy)(bpy)(py)^{2+}$ (585 nm) in 77 K frozen acetonitrile solution is shifted by ~2000 cm^{-1} from that of $Ru(tpy)(bpy)(Cl)^+$ (662 nm).[62] Thus, we propose that the lowest excited state has less, but not inconsequential, ^{3}MLCT character. For example, variations in the extent of MLCT mixing also are suggested by the fact that values of S (1.3−1.4) for **2**−**4** are slightly greater than that for **1** (1.0; Figure 5b and Table 3).

Table 3. Emission Spectroscopic Data for Pt(phebox)Cl and 1−8 in 77 K Ethanol−Methanol (4:1) Glassy Solution (λ_{ex} = 350 nm)

compound	emission (λ_{max}, nm)	$I_{0,0}/I_{1,0}$ (S)
1	497, 537, 586, 640	1.0
2a[a]	484, 523, 572, 628	1.4
3[a]	489, 526, 572, 628	1.4
4[a]	485, 523, 570, 627	1.3
5[a]	390, 414, 441, 465, 497, 533, 584, 638, 657sh	
6	487, 522, 566, 619	1.4
7a	490, 528, 572, 626	1.4
8	486, 528, 572, 626	1.4

[a]With >50 equiv of pyridyl ligand.

Note that the excitation spectrum of Pt(phebox)Cl, which is in good agreement with the absorption spectrum (Figure 5b), also shows two weak low-energy features near 460 and 490 nm (1300 cm^{-1} spacing). Similar features appear in the 77 K excitation spectrum of $Pt(tpy)Cl^+$ (433, 464 nm)[83] and the absorption spectrum of Pt(bpb)Cl (485 nm, 145 M^{-1} cm^{-1}).[39] The narrow, lower-energy feature overlaps well with the first vibronic feature at 497 nm in the emission spectrum. Accordingly, we assign this absorption to the lowest-energy spin-forbidden mainly ^{3}LC transition.

From these results and based on the shortest wavelength emission vibronic band, we can draw conclusions concerning the relative energies of the lowest excited states of Pt(tpy)Cl (77 K, butyronitrile, 470 nm),[67] Pt(bpb)Cl (RT, CH_2Cl_2, 491 nm; 77 K, 2-methyl-tetrahydrofuran, 486 nm),[41] Pt(phebox)Cl (RT, CH_2Cl_2, 510 nm; 4:1 EtOH/MeOH 497 nm), and Pt(bib)Cl (RT, CH_2Cl_2, 562 nm). The accumulated data suggest that the energy decreases along the series $Pt(tpy)Cl^+$ > Pt(bpb)Cl > Pt(phebox)Cl > Pt(bib)Cl. The experimental data contradict estimates from DFT calculations, which suggest $Pt(bpb)Cl > Pt(tpy)Cl^+$.[84] The states for $Pt(tpy)Cl^+$, Pt(bpb)Cl, and Pt(phebox)Cl lie within a narrow range (~1200 cm^{-1}), whereas that of Pt(bib)Cl is stabilized by ~1800 cm^{-1} (~0.2 eV) below that of Pt(phebox)Cl. The destabilization of the lowest excited state of **1** as compared to Pt(bib)Cl is qualitatively consistent with the electron donor properties of the oxazolinyl ether group, which is expected to have a destabilizing influence on the lowest $phebox^-$ π^* level and therefore reduce MLCT character in the lowest excited state.

Compound **5** with excess acridine exhibits three emission bands in 77 K frozen solution (Figure S10). The shorter wavelength progression matches that of free acridine under these conditions, whereas the midrange progression (495, 533, 584, 638 nm) is similar to that of Pt(phebox)Cl. Interestingly, at longer wavelengths there is unexpected additional intensity and a distinct shoulder at 657 nm, which are consistent with acridine phosphorescence.[85] It is possible that the latter originates from the $Pt(phebox)(ac)^+$ complex or energy transfer to free acridine.

DOI: 10.1021/acs.inorgchem.5b01022
Inorg. Chem. XXXX, XXX, XXX−XXX

CONCLUSIONS

To place these findings in context, it is useful to compare the preceding observations with those obtained for the Pt(pip$_2$NCN)L^{n+} analogues. Notably, the latter give rise to emissions in frozen solution from lowest ^{3}LF, pyridyl ^{3}LC, or ^{3}MLCT states involving the pyridyl ligand. By contrast, and as a result of the low-lying π^*(phebox$^-$) level, **1**−**4** and **6**−**8** give rise to emissions from distinctly different lowest excited states having ^{3}LC and ^{3}MLCT character involving the phebox$^-$ ligand (Figure 5b and Figure S11). Thus, subtle variations in the nature of the NCN and ancillary ligands provide access to at least five orbitally distinct emissive excited states. Interestingly and as also evident for Pt(bpb)Cl[39−41] and Pt(bib)Cl,[38] the LC and MLCT states involving the NCN ligand are much less susceptible to nonradiative deactivation in fluid solution than Pt(pip$_2$NCN)L^{n+} complexes. Likewise, although Pt(tpy)L^{n+} complexes have lowest excited states with tpy LC/MLCT character, those complexes tend to be nonemissive in fluid solution due to population of low-lying LF states resulting in nonradiative deactivation.[86,87] Thus, it would appear that the strong donor properties of the phenyl donor groups of phebox$^-$, bpb$^-$, and bib$^-$ ligands increase the gap between the lowest state and higher-lying LF states, thereby reducing the latter's deactivating effect. Lastly, we note that, for chloro complexes with different meridional tridentate ligands, we have found that the lowest excited-state energy decreases along the series Pt(tpy)Cl$^+$ > Pt(bpb)Cl > Pt(phebox)Cl > Pt(bib)Cl. Taken all together, the results presented here suggest a rather synthetically convenient means of modulating the orbital character and energies of the lowest excited states of platinum(II) complexes with the 1,3-bis(imino)benzene ligand skeleton.

ASSOCIATED CONTENT

Supporting Information

The Supporting Information is available free of charge on the ACS Publications website at DOI: 10.1021/acs.inorgchem.5b01022. CCDC Nos. 1058633−1058642 contain the crystallographic data for **1**, **2b**, **3-m**, **3-o**, **4**−**6**, **7b**, **8-c**, and **8-p**. These data can be obtained free of charge from the Cambridge Data Centre via www.ccdc.cam.ac.uk/data_request/cif.

Synthesis details, complete details of the crystallographic study, tables of selected bond distances and angles, oxazolinyl puckering analysis, analytical and spectroscopic data, and ^{1}H NMR spectra of **2** during titration with pyridine. (PDF)

AUTHOR INFORMATION

Corresponding Author

*E-mail: bill.connick@uc.edu. Fax: (+1) 513-556-9239.

Notes

The authors declare no competing financial interest.

ACKNOWLEDGMENTS

This research was supported the National Science Foundation (Grant No. CHE-1152853). Funding for the SMART6000 CCD diffractometer was through NSF-MRI Grant No. CHE-0215950. D.Z. thanks the Univ. of Cincinnati Univ. Research Council for a summer fellowship. We also thank Drs. L. Sallans and S. Macha for assistance with MS measurements. Synchrotron data were collected through the Service Crystallography at Advanced Light Source (SCrALS) project at Beamline 11.3.1 at the Advanced Light Source (ALS), Lawrence Berkeley National Laboratory. The ALS is supported by the U.S. Department of Energy, Office of Energy Sciences, under Contract No. DE-AC02-05CH11231.

REFERENCES

(1) van Koten, G. *Top. Organomet. Chem.* **2013**, *40*, 1−20.
(2) Nishiyama, H.; Ito, J.-i. *Chem. Commun.* **2010**, *46*, 203−212.
(3) Nishiyama, H. *Chem. Soc. Rev.* **2007**, *36*, 1133−1141.
(4) Motoyama, Y.; Okano, M.; Narusawa, H.; Makihara, N.; Aoki, K.; Nishiyama, H. *Organometallics* **2001**, *20*, 1580−1591.
(5) Motoyama, Y.; Makihara, N.; Mikami, Y.; Aoki, K.; Nishiyama, H. *Chem. Lett.* **1997**, 951−952.
(6) Motoyama, Y.; Narusawa, H.; Nishiyama, H. *Chem. Commun.* **1999**, 131−132.
(7) Motoyama, Y.; Nishiyama, H. *Synlett* **2003**, 1883−1885.
(8) Motoyama, Y.; Koga, Y.; Nishiyama, H. *Tetrahedron* **2001**, *57*, 853−860.
(9) Motoyama, Y.; Koga, Y.; Kobayashi, K.; Aoki, K.; Nishiyama, H. *Chem. - Eur. J.* **2002**, *8*, 2968−2975.
(10) Fossey, J. S.; Richards, C. J. *J. Organomet. Chem.* **2004**, *689*, 3056−3059.
(11) Stol, M.; Snelders, D. J. M.; Godbole, M. D.; Havenith, R. W. A.; Haddleton, D.; Clarkson, G.; Lutz, M.; Spek, A. L.; van Klink, G. P. M.; van Koten, G. *Organometallics* **2007**, *26*, 3985−3994.
(12) Bugarin, A.; Connell, B. T. *Organometallics* **2008**, *27*, 4357−4369.
(13) Inoue, H.; Kikuchi, M.; Ito, J.-i.; Nishiyama, H. *Tetrahedron* **2008**, *64*, 493−499.
(14) Mizuno, M.; Inoue, H.; Naito, T.; Zhou, L.; Nishiyama, H. *Chem. - Eur. J.* **2009**, *15*, 8985−8988.
(15) Tsuchiya, Y.; Uchimura, H.; Kobayashi, K.; Nishiyama, H. *Synlett* **2004**, 2099−2102.
(16) Kanazawa, Y.; Nishiyama, H. *Synlett* **2006**, 3343−3345.
(17) Kanazawa, Y.; Tsuchiya, Y.; Kobayashi, K.; Shiomi, T.; Itoh, J.; Kikuchi, M.; Yamamoto, Y.; Nishiyama, H. *Chem. - Eur. J.* **2006**, *12*, 63−71.
(18) Tsuchiya, Y.; Kanazawa, Y.; Shiomi, T.; Kobayashi, K.; Nishiyama, H. *Synlett* **2004**, 2493−2496.
(19) Stark, M. A.; Jones, G.; Richards, C. J. *Organometallics* **2000**, *19*, 1282−1291.
(20) Motoyama, Y.; Kawakami, H.; Shimozono, K.; Aoki, K.; Nishiyama, H. *Organometallics* **2002**, *21*, 3408−3416.
(21) Denmark, S. E.; Stavenger, R. A.; Faucher, A.-M.; Edwards, J. P. *J. Org. Chem.* **1997**, *62*, 3375−3389.
(22) Stark, M. A.; Richards, C. J. *Tetrahedron Lett.* **1997**, *38*, 5881−5884.
(23) Ito, J.-i.; Ujiie, S.; Nishiyama, H. *Chem. Commun.* **2008**, 1923−1925.
(24) Williams, J. A. G. *Chem. Soc. Rev.* **2009**, *38*, 1783−1801.
(25) Li, K.; Chen, Y.; Lu, W.; Zhu, N. Y.; Che, C. M. *Chem. - Eur. J.* **2011**, *17*, 4109−4112.
(26) Albrecht, M.; van Koten, G. *Angew. Chem., Int. Ed.* **2001**, *40*, 3750−3781.
(27) van der Boom, M. E.; Milstein, D. *Chem. Rev.* **2003**, *103*, 1759−1792.
(28) Jude, H.; Krause Bauer, J. A.; Connick, W. B. *Inorg. Chem.* **2002**, *41*, 2275−2281.
(29) Jude, H.; Krause Bauer, J. A.; Connick, W. B. *Inorg. Chem.* **2004**, *43*, 725−733.
(30) Jude, H.; Krause Bauer, J. A.; Connick, W. B. *Inorg. Chem.* **2005**, *44*, 1211−1220.
(31) Shi, L.-L.; Liao, Y.; Yang, G.-C.; Su, Z.-M.; Zhao, S.-S. *Inorg. Chem.* **2008**, *47*, 2347−2355.
(32) Batema, G. D.; van de Westelaken, K. T. L.; Guerra, J.; Lutz, M.; Spek, A. L.; van Walree, C. A.; de Mello Donega, C.; Meijerink, A.; van

DOI: 10.1021/acs.inorgchem.5b01022
Inorg. Chem. XXXX, XXX, XXX−XXX

Klink, G. P. M.; van Koten, G. *Eur. J. Inorg. Chem.* **2007**, *2007*, 1422−1435.
(33) Motoyama, Y.; Mikami, Y.; Kawakami, H.; Aoki, K.; Nishiyama, H. *Organometallics* **1999**, *18*, 3584−3588.
(34) Fossey, J. S.; Richards, C. J. *Organometallics* **2004**, *23*, 367−373.
(35) Ito, J.-i.; Ujiie, S.; Nishiyama, H. *Organometallics* **2009**, *28*, 630−638.
(36) Chuchuryukin, A. V.; Huang, R.; Lutz, M.; Chadwick, J. C.; Spek, A. L.; van Koten, G. *Organometallics* **2011**, *30*, 2819−2830.
(37) Stol, M.; Snelders, D. J. M.; de Pater, P. J. J. M.; van Klink, K. G. P. M.; Kooijman, H.; Spek, A. L.; van Koten, G. *Organometallics* **2005**, *24*, 743−749.
(38) Blackburn, O. A.; Coe, B. J.; Helliwell, M.; Raftery, J. *Organometallics* **2012**, *31*, 5307−5320.
(39) Williams, J. A. G.; Beeby, A.; Davies, E. S.; Weinstein, J. A.; Wilson, C. *Inorg. Chem.* **2003**, *42*, 8609−8611.
(40) Farley, S. J.; Rochester, D. L.; Thompson, A. L.; Howard, J. A. K.; Williams, J. A. G. *Inorg. Chem.* **2005**, *44*, 9690−9703.
(41) Wang, Z.; Turner, E.; Mahoney, V.; Madakuni, S.; Groy, T.; Li, J. *Inorg. Chem.* **2010**, *49*, 11276−11286.
(42) Sotoyama, W.; Satoh, T.; Sato, H.; Matsuura, A.; Sawatari, N. *J. Phys. Chem. A* **2005**, *109*, 9760−9766.
(43) Chen, Y.; Lu, W.; Che, C.-M. *Organometallics* **2013**, *32*, 350−353.
(44) Elguero, J.; Gonzalez, E.; Imbach, J. L.; Jacquier, R. *Bull. Soc. Chim. Fr.* **1969**, *11*, 4075−4077.
(45) Frenna, V.; Vivona, N.; Consiglio, G.; Spinelli, D. *J. Chem. Soc., Perkin Trans. 2* **1985**, 1865−1868.
(46) Kissinger, P. T.; Heineman, W. R. *J. Chem. Educ.* **1983**, *60*, 702−706.
(47) Harris, T. D.; Neuschwander, B.; Boekelheide, V. *J. Org. Chem.* **1978**, *43*, 727−730.
(48) Button, K. M.; Gossage, R. A.; Phillips, R. K. R. *Synth. Commun.* **2002**, *32*, 363−368.
(49) Fossey, J. S.; Jones, G.; Motevalli, M.; Nguyen, H. V.; Richards, C. J.; Stark, M. A.; Taylor, H. V. *Tetrahedron: Asymmetry* **2004**, *15*, 2067−2073.
(50) Han, Y.; Huynh, H. V.; Tan, G. K. *Organometallics* **2007**, *26*, 6447−6452.
(51) Stang, P. J.; Cao, D. H.; Saito, S.; Arif, A. M. *J. Am. Chem. Soc.* **1995**, *117*, 6273−6283.
(52) Komeda, S.; Kalayda, G. V.; Lutz, M.; Spek, A. L.; Yamanaka, Y.; Sato, T.; Chikuma, M.; Reedijk, J. *J. Med. Chem.* **2003**, *46*, 1210−1219.
(53) Willermann, M.; Mulcahy, C.; Sigel, R. K. O.; Cerda, M. M.; Freisinger, E.; Sanz Miguel, P. J.; Roitzsch, M.; Lippert, B. *Inorg. Chem.* **2006**, *45*, 2093−2099.
(54) Janzen, D. E.; Patel, K. N.; VanDerveer, D. G.; Grant, G. J. *Chem. Commun.* **2006**, 3540−3542.
(55) Sawada, T.; Yoshizawa, M.; Sato, S.; Fujita, M. *Nat. Chem.* **2009**, *1*, 53−56.
(56) Hirahara, E.; Takaishi, S.; Yamashita, M. *Chem. - Asian J.* **2009**, *4*, 1442−1450.
(57) Rao, Y. L.; Wang, S. N. *Inorg. Chem.* **2009**, *48*, 7698−7713.
(58) Sun, S. S.; Anspach, J. A.; Lees, A. J.; Zavalij, P. Y. *Organometallics* **2002**, *21*, 685−693.
(59) Albrecht, M.; Lutz, M.; Schreurs, A. M. M.; Lutz, E. T. H.; Spek, A. L.; van Koten, G. *J. Chem. Soc. Dalton.Trans.* **2000**, 3797−3804.
(60) Chuchuryukin, A. V.; Chase, P. A.; Mills, A. M.; Lutz, M.; Spek, A. L.; van Klink, G. P. M.; van Koten, G. *Inorg. Chem.* **2006**, *45*, 2045−2054.
(61) Hill, M. G.; Bailey, J. A.; Miskowski, V. M.; Gray, H. B. *Inorg. Chem.* **1996**, *35*, 4585−4590.
(62) Tsai, C. N.; Allard, M. M.; Lord, R. L.; Luo, D. W.; Chen, Y. J.; Schlegel, H. B.; Endicott, J. F. *Inorg. Chem.* **2011**, *50*, 11965−11977.
(63) Juris, A.; Balzani, V.; Barigelletti, F.; Campagna, S.; Belser, P.; von Zelewsky, A. *Coord. Chem. Rev.* **1988**, *84*, 85−277.
(64) Rossi, E.; Murphy, L.; Brothwood, P. L.; Colombo, A.; Dragonetti, C.; Roberto, D.; Ugo, R.; Cocchi, M.; Williams, J. A. G. *J. Mater. Chem.* **2011**, *21*, 15501−15510.
(65) Mroz, W.; Botta, C.; Giovanella, U.; Rossi, E.; Colombo, A.; Dragonetti, C.; Roberto, D.; Ugo, R.; Valore, A.; Williams, J. A. G. *J. Mater. Chem.* **2011**, *21*, 8653−8661.
(66) Komorsky-Lovric, S.; Mirceski, V.; Scholz, F. *Microchim. Acta* **1999**, *132*, 67−77.
(67) Michalec, J. F.; Bejune, S. A.; Cuttell, D. G.; Summerton, G. C.; Gertenbach, J. A.; Field, J. S.; Haines, R. J.; McMillin, D. R. *Inorg. Chem.* **2001**, *40*, 2193−2200.
(68) Ball, P. J.; Shtoyko, T. R.; Krause Bauer, J. A.; Oldham, W. J.; Connick, W. B. *Inorg. Chem.* **2004**, *43*, 622−632.
(69) Halverson, F.; Hirt, A. R. C. *J. Chem. Phys.* **1951**, *19*, 711−718.
(70) Krumholz, P. *J. Am. Chem. Soc.* **1951**, *73*, 3487−3492.
(71) Favini, G. *Gazz. Chim. Ital.* **1963**, *93*, 635−648.
(72) Tastan, S.; Krause, J. A.; Connick, W. B. *Inorg. Chim. Acta* **2006**, *359*, 1889−1898.
(73) Ryu, C. K.; Kyle, K. R.; Ford, P. C. *Inorg. Chem.* **1991**, *30*, 3982−3986.
(74) Giordano, P. J.; Wrighton, M. S. *J. Am. Chem. Soc.* **1979**, *101*, 2888−2897.
(75) Yip, H. K.; Che, C. M.; Peng, S. M. *J. Chem. Soc., Dalton Trans.* **1993**, 179−187.
(76) Da, T. T.; Vu, D. B.; Dinh, N. H. *J. Coord. Chem.* **2004**, *57*, 485−496.
(77) Turnbull, N. H. *J. Chem. Soc.* **1945**, 441−444.
(78) Fleeman, W. L.; Connick, W. B. *Comments Inorg. Chem.* **2002**, *23*, 205−230.
(79) Connick, W. B.; Miskowski, V. M.; Houlding, V. H.; Gray, H. B. *Inorg. Chem.* **2000**, *39*, 2585−2592.
(80) Connick, W. B.; Geiger, D.; Eisenberg, R. *Inorg. Chem.* **1999**, *38*, 3264−3265.
(81) Wilson, M. H.; Ledwaba, L. P.; Field, J. S.; McMillin, D. R. *Dalton Trans.* **2005**, 2754−2759.
(82) The excitation spectra for **2**−**8** are consistent with the absorption spectra and support the conclusion that the emissions originate from different chromophores rather than, for example, a shared impurity.
(83) Bailey, J. A.; Hill, M. G.; Marsh, R. E.; Miskowski, V. M.; Schaefer, W. P.; Gray, H. B. *Inorg. Chem.* **1995**, *34*, 4591−4599.
(84) Shi, L. L.; Li, T.; Zhao, S. S.; Li, H.; Su, Z. *Theor. Chem. Acc.* **2009**, *124*, 29−36.
(85) Morawski, O.; Prochorow, J. *Chem. Phys. Lett.* **1995**, *242*, 253−258.
(86) Miskowski, V. M.; Houlding, V. H.; Che, C. M.; Wang, Y. *Inorg. Chem.* **1993**, *32*, 2518−2524.
(87) Aldridge, T. K.; Stacy, E. M.; McMillin, D. R. *Inorg. Chem.* **1994**, *33*, 722−727.

DOI: 10.1021/acs.inorgchem.5b01022
Inorg. Chem. XXXX, XXX, XXX−XXX